Dynamics and stability of racing boats with air wings

Nikolai Kornev* and Lutz Kleinsorge

Department of Mechanical Engineering and Naval Architecture,
University of Rostock,
Albert-Einstein-Str. 2, 18051 Rostock,
Germany Rostock, Germany
E-mail: Nikolai.Kornev@uni-rostock.de
E-mail: Lutz.Kleinsorge@uni-rostock.de
*Corresponding author

Günther Migeotte

ICARUS Design AS,
Titangaten Gaten 1,
1630 Gamle Fredriskstad, Norway
E-mail: gunther.migeotte@gmail.com

Abstract: The aim of this paper is to derive a mathematical model for predicting the longitudinal stability of racing boats with aerodynamic support. The theory is based on a combination of stability theories developed for planing boats and wing in ground effect craft. The influence of different geometric and mass boat parameters on the stability is investigated.

Keywords: longitudinal stability; racing boats; wing in ground effect.

Reference to this paper should be made as follows: Kornev, N., Kleinsorge, L. and Migeotte, G. (2010) 'Dynamics and stability of racing boats with air wings', *Int. J. Aerodynamics*, Vol. 1, No. 1, pp.28–51.

Biographical notes: Nikolai Kornev completed his BS in 1984 at Marine Technical University St. Petersburg. He received his PhD (Candidate of Science) in Ship Theory in 1988 and second PhD (Doctor of Science) in Fuid Mechanics in 1998. He has been involved in the theoretical works supporting the development of Russian and German WIG craft and planing ships. Since 2003, he has been a Professor of Mechanical Engineering at the University of Rostock (Germany). His research interests include CFD, ship theory, heat and mass transfer.

Lutz Kleinsorge is a student of Naval Architecture from the University of Rostock (Germany). His main interests include ship theory and fluid dynamics. He will graduate in 2009 with the topic on mesh generation for numerical ship flow calculation using LES.

Günther Migeotte is a graduate of Naval Architecture from the University of Stellenbusch (South Africa). He received his PhD with the topic on hydrofoil assisted catamarans in 2001. Thereafter, he works as the Director and Chief Engineer for several companies, always with the main focus on hull design of high speed craft of various types, including monohulls, catamarans, trimarans, stepped hulls and hydrofoils. Most of the boats he designed are for speeds above 40 knots and up to 120 knots (racing catamarans).

1 Introduction

Since the inception of planing hulls, speeds of racing boats have been increasing from a speed of about 50 knots half a century ago to speed of 150 knots+ that are common place today with modern planing boats, see Figure 1. With continuously increasing speed, stability of these craft has become a more important consideration. The International Towing Tank Conference (ITTC) has identified the following different forms of instability that affect high speed planing craft:

- takeoff
- loss of GM due to wave system
- course keeping and lateral stability
- bow diving and plough-in
- porpoising
- chine tripping
- spray rail engulfing resulting in plough-in
- effect of critical speed in shallow water.

Figure 1 Racing boat Qatar

Source: http://www.class-1.com

Most of these different forms of instability are well-understood and/or mathematical models exist for predicting the onset of such instabilities and The Specialist Committee of High-Speed Marine Vehicles (2001) gives a good list of reference works on each

of these instabilities. Notably however, the problem of takeoff, which is normally associated with very high speed catamarans, has according to the ITTC not been well-addressed to date. Figure 2 shows a series of video stills taken from the internet (http://www.youtube.com) of an Offshore Class-1 catamaran pitching-up and then taking off that illustrates the severity and danger of this form of instability.

Figure 2 Crash due to loss of the longitudinal stability (see online version for colours)

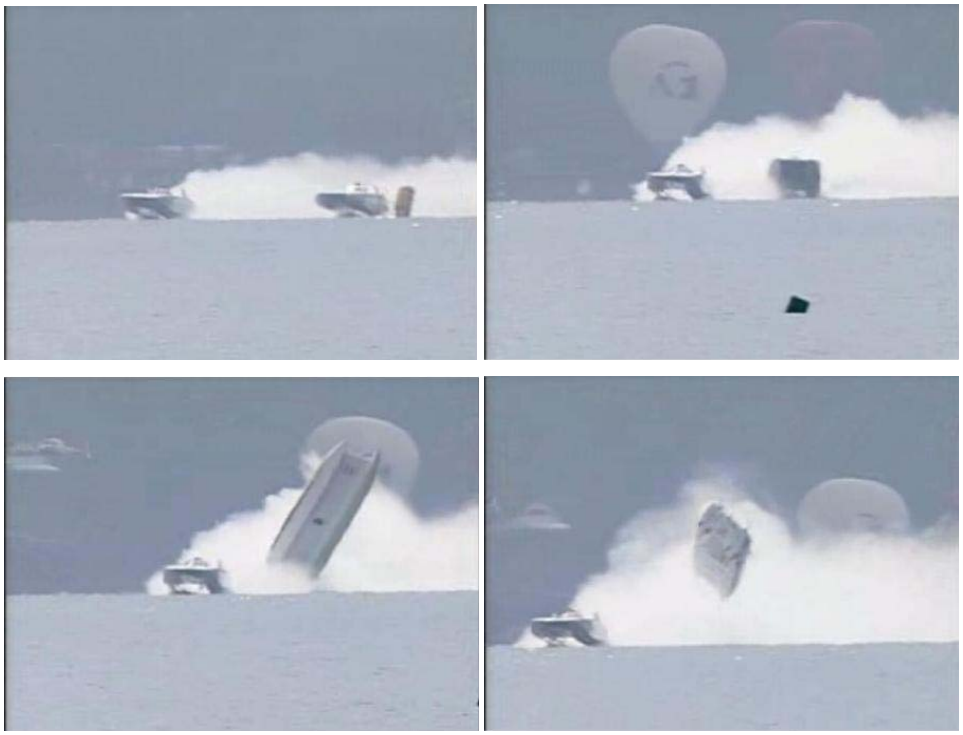

Source: http://www.youtube.com

There is a very fine balance between the aerodynamic, hydrodynamic and propulsive forces at the high speeds the boats travel at (up to 200 knots for some hydroplanes). This is especially true for planing vessels that make use of significant aerodynamic lift such as catamarans. The stability can be easily upset by waves, wind gusts and turning (asymmetrical flow). Instability is usually onset due to a pitch-up motion that results in the hull taking off and pitching about the propeller. Once airborne, the vessel quickly flies out of control often with catastrophic consequences as indicated in Figure 2. Englar et al. (1995) have studied this form of instability for racing hydroplanes.

The primary design consideration of such catamarans is usually high speed. Analysis of the resistance characteristics of the vessels shows that the lowest resistance, and the highest speed, is obtained by maximising the aerodynamic lift while keeping the hydrodynamic forces to a minimum. When considering the balance of forces and moments (see Section 2), it is clear that the aerodynamic forces are the source of the instability of such boats as the centre of aerodynamic lift is located ahead of the longitudinal centre of gravity (LCG) of the boat. Thus, increasing the aerodynamic lift

component is inherently coupled with decreasing stability of the boat. The design of such vessels is therefore a compromise between aero- and hydrodynamic considerations and retaining a fine balance between the various parameters that influence the stability. At present, the stability of these vessels is usually evaluated using simple balance of moments and some simple design rules (see Russel, 2007). Such simple methods are, however, inadequate to ensure stability as pitch-up and takeoff stability remains an important problem and is the cause of many accidents.

Takeoff and pitch tendencies are strongly associated with the aerodynamics of such hulls and are therefore only a consideration when the aerodynamic lift produced becomes a significant portion of the total lift. Typically, this occurs at Froude numbers, $Fn_\nabla = \frac{V}{\sqrt{g\nabla^{0.333}}} > 7.0$ which represents speeds in excess of 60 knots for most of the craft in operation today. The stability of such craft is similar to the takeoff stability of wing in ground (WIG) craft and in essence the same methods can be applied to determine the stability of catamarans. Morch (2003) discussed some details of the aero- and hydrodynamics of very high speed catamarans (80 knots), but a discussion of stability is not given. The results of his experiments and computational fluid dynamics (CFD) computations however indicate that, for the 7.5 m catamaran travelling at 80 knots he investigated, the aerodynamic lift forces were over 50% during normal operation of the craft and that the centre of aerodynamic lift is very sensitive to the running trim angle of the vessel.

The most common way to increase speed on such high speed catamarans is to run at a higher trim angle, but this brings the vessel closer to its stability limits and often such crafts run in a marginally unstable condition with the pilot providing continuous correction to the running attitude. Constant vigilance is therefore required by the pilot to prevent the boat from taking off. Such boats often include some emergency measures such as water ballast tanks in the bows that can be filled with water in a very short time if the boat cannot be controlled and wants to takeoff.

The critical nature of the stability of these crafts is evident. Proper design tools in order to analyse stability of such crafts would be valuable to be able to develop designs that can possibly extend the operable limits of these crafts further. A longitudinal theory is proposed below which meets this requirement. The theory is based on two theoretical developments. The first development is the stability theory of planing boats proposed in a series of theoretical and experimental works performed during more than two decades during the ‘60s and ‘70s at the Central Aero-Hydrodynamic Institute (TSAGI) in the USSR. The most valuable achievement is the simple and very robust mathematical model for the calculation of hydrodynamic forces acting on a planing surface at both steady and unsteady flow conditions. This model has been thoroughly tested in various measurements by Kovrizhnykh (1978). Implementation of this model, within linear stability theory, results in a fourth order characteristic equation that has a couple of conjugate roots. Kovrizhnykh (1978) and Lotov (1984) have showed that oscillatory instability is the most serious problem for the planing boats, whereas the aperiodic instability has never been observed. Kovrizhnykh obtained the areas of planing boat instability. At a given speed, the stability gets worse as the angle of attack increases. The planing boat becomes unstable when the angle of attack attains a definite critical value. Surprisingly, there is a narrow area of stability at large angles of attack which quickly disappears when the angle gets even larger. The presence of this stability region is confirmed in measurements with freely towed planing boat models by Tikhonov (1961).

Figure 3 Coordinate system

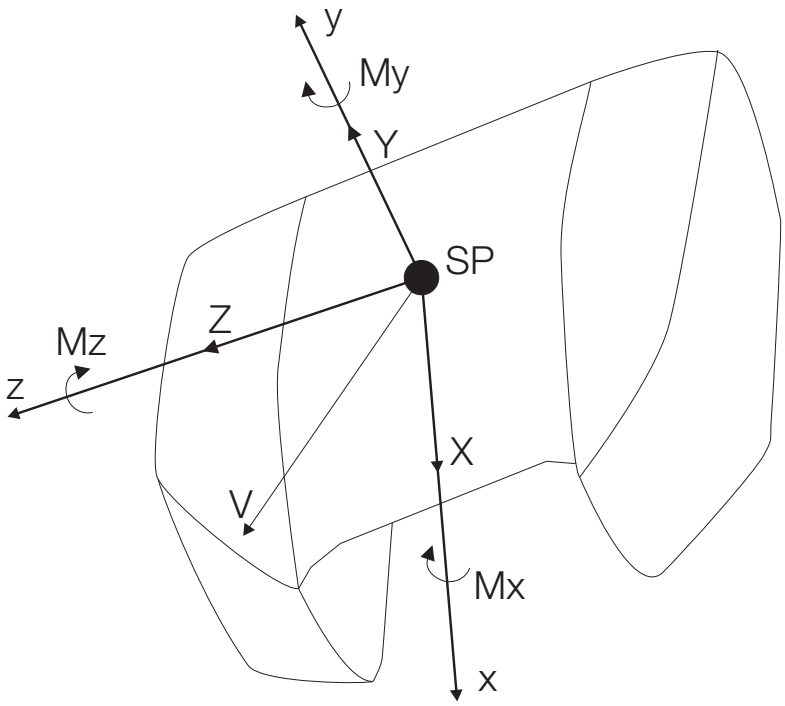

The second development used in the present paper concerns WIG craft. With the development of WIG craft and ekranoplans in the USSR, much work was done on the stability of high speed craft making use of aerodynamic support (see Zhukov, 1993). Both the lateral and longitudinal stability of WIG craft had been thoroughly tested and well-understood. In this paper, we restrict ourselves to the longitudinal stability theory for WIG craft as developed by Irodov (1970) and independently by Staufenbiel (1987) in Germany. They derived the criterion of the static stability in two different forms, but with the same physical meaning. Both criteria can be reduced to the same form after simple algebraic transformations. According to Irodov, a WIG craft is statically stable when the aerodynamic centre in height $x_h = m_z^h / C_y^h$ lies in front of the aerodynamic centre in pitch $x_\vartheta = m_z^\vartheta / C_y^\vartheta$ where h is the height of flight, ϑ the pitch angle, C_y and m_z are respectively the lift coefficient and the pitching moment coefficient, and $C_y^{\vartheta,h}$ and $m_z^{\vartheta,h}$ are their derivatives. According to experience, if the criterion of the static stability referred to the mean aerodynamic chord is between 0.05 and 0.12, the statically stable WIG craft is stable dynamically as well. Excessive static stability can result in dynamic instability. A weak positive static stability is not admissible because of too weak damping of perturbations. Another important requirement widely used in the design of Russian WIG craft is the reciprocal position of aerodynamic centres and centre of mass of the vehicle. The LCG should be located between both aerodynamic centres x_h and x_ϑ closer to the aerodynamic centre in height x_h (Zhukov, 1993). In this case, the dynamical properties of the WIG craft are favourable and the response of the craft to perturbations is mild. The longitudinal dynamic stability is investigated using three equations describing

the translatory motions in x and y directions and pitching motions, see Figure 3. The procedure which is usual in linear stability analysis leads to the characteristic equation of the fifth order which has one real root and a couple of two conjugate roots. A typical mutual position of roots for the stable WIG craft is presented in Benedikt et al. (2001). The most important is the couple with the minimal real part which is responsible for the appearance of the dynamic oscillatory instability.

These two stability theories are used in this paper for developing the complex stability theory of planing craft with aerodynamic support. A part of this work has been presented at the 6th International Conference on High-Performance Marine Vehicles (HIPER 08) in Italy (Kornev et al., 2008).

2 Theory of longitudinal stability

2.1 Steady equilibrium condition

A necessary requirement for stability is that the planing boat is in an equilibrium condition. This means that the sum of vertical forces has to be zero:

$$mg - \left(Y_0 + C_y \frac{\rho}{2} U_a^2 S \right) = 0 \tag{1}$$

where Y_0 is the steady hydrodynamic lift evaluated in Section 2.4. The moment around the z axis can be neglected because equilibrium of moments can be easily derived for every operation point by an interceptor or an elevator unit. Equation (1) is used to determine the floating position (draught) of a racing boat at a given speed and trim angle.

2.2 Motion equations

When the steady equilibrium condition is fulfilled, the stability is determined through analysis of roots of the characteristic equation derived from a linearised equation system describing the longitudinal perturbed motion.

Equations of three-dimensional dynamics of racing boats can be obtained directly from the second law of Newton and can be stated in fixed, speed, connected or semi-connected coordinate system (see Plisov et al., 1991) (Figure 3). For formulation of the dynamics equations, the choice of coordinate system is defined by requirements of simplicity of form and convenience in presentation of forces. Most appropriate in this sense is the semi-connected system of coordinates.

A complete system of equations of three-dimensional motion is (designations see in Table 1 and Figure 4):

$$\dot{U}_d = f_1 T - f_2 U_a^2 \left(C_x - C_z \beta_a \right) - f_1 R_{x,hydr}(t)$$

$$\dot{U}_{ycg} = f_2 U_a^2 C_y + f_1 T \vartheta_T - 9.81 + f_1 R_{y,hydr}(t)$$

$$\dot{\beta}_d = f_2 U_a \left(C_z + C_y \gamma + C_x \beta_a \right) + \omega_y - T \beta_a$$

$$\dot{\omega}_x = f_3 U_a^2 \left(m_x + f_4 m_y \right)$$

$$\dot{\omega}_y = f_5 U_a^2 \left(m_y - f_6 m_x \right)$$

$$\dot{\omega}_z = \left(f_7 U_a^2 m_z - f_8 T \right) + \frac{m_{z,hydr}(t)}{J_z}$$

Table 1 Nomenclature

b	$[m]$	Chord of the wing
C_x		Aerodynamic drag coefficient
C_y		Aerodynamic lift coefficient
C_z		Aerodynamic side force coefficient
C_T^U		Derivative of thrust coefficient on speed
C_W		Coefficient of hydrodynamic resistance
g	$[m/s^2]$	Acceleration of gravity
H	$[m]$	Submergence of the boat under centre of gravity
H_0	$[m]$	Submergence at the transom of the racing boat
h	$[m]$	Height of flight
h_{cg}	$[m]$	Height of centre of mass
h_t	$[m]$	Height of the boat at the transom
$J_x;\ J_y;\ J_z$	$[k/gm^2]$	Mass moment of inertia
$k(\beta)$		Coefficient of added mass
L	$[m]$	Span of the wing
l_0	$[m]$	Wetted length of the hull
LCG	$[m]$	Longitudinal position of centre of gravity, measured from the transom of the boat
m_0	$[kg]$	Mass
$m_{hull};\ m_{wing}$	$[kg]$	Masses of estimation of J_z
m_{hydr}	$[kg]$	Added mass of planing boat cross-section
$m_x;\ m_y;\ m_z$		Coefficients of aerodynamic moments around x, y and z axes
$m_{z,hydr}(t)$	$[Nm]$	Trim hydrodynamic moment
M_W	$[Nm]$	Trim moment of hydrodynamic resistance

Table 1 Nomenclature (continued)

$R_{x,hydr}(t)$	$[N]$	Hydrodynamic drag force
$R_{y,hydr}(t)$	$[N]$	Hydrodynamic lift force
S	$[m^2]$	Area of the wing
S_0	$[m^2]$	Wetted surface of the hull
$S_{wing};\ S_{hull}$	$[m^2]$	Areas for estimation of J_z
T	$[N]$	Thrust of the boat
U_a	$[m/s]$	Boat speed with wind perturbations
U_d	$[m/s]$	Boat speed
U_{ycg}	$[m/s]$	Velocity of centre of gravity in vertical direction
$x_{cg};\ y_{cg}$	$[m]$	Position of centre of gravity
Y_0	$[N]$	Steady hydrodynamic lift
y_T	$[m]$	Thrust arm of the engine
W	$[N]$	Hydrodynamic resistance
$w_x;\ w_y;\ w_z$	$[ms^{-1}]$	Wind perturbations
α		$\vartheta_0 + \vartheta$
β		Deadrise angle
β_a	$[rad]$	Drift angle with wind perturbations
β_d	$[rad]$	Drift angle
ψ	$[rad]$	Angle of course
γ	$[rad]$	Angle of roll
λ		Aspect ratio of the air wing
$u;\ i_z$		Dimensionless mass and mass moment of inertia
η_0	$[m]$	Distance between keel and centre of gravity
ρ	$[kg/m^3]$	Density of air
ρ_W	$[kg/m^3]$	Density of water
θ_T	$[rad]$	Setup angle of the engine
ϑ	$[rad]$	Pitch or trim angle
ϑ_0	$[rad]$	Mean trim angle
ξ_0	$[m]$	Distance between stern and centre of gravity
$\omega_x;\ \omega_y;\ \omega_z$	$[1/s]$	Angular velocities

Figure 4 Main dimensions of planing boat

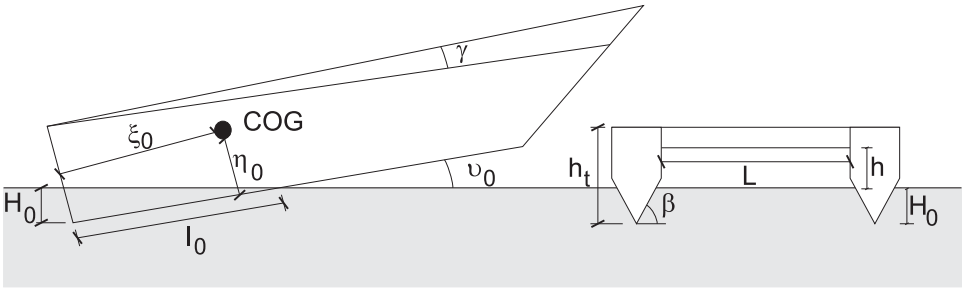

For formulation of the equations, additional parameters are used:

$$\dot{h}_{cg} = U_{y_{cg}}, \quad \dot{\gamma} = \omega_x - \omega_y\left(\vartheta - \vartheta_0\right), \quad \dot{\psi} = \omega_y, \quad \dot{\vartheta} = \omega_z$$

$$\beta_a = \beta_d - \frac{w_z(t)}{U_a}, \quad U_y = U_{y_{cg}} - w_y(t), \quad U_a = U_d + w_x(t)$$

$$\psi_d = \psi - \beta_d, \quad h = \frac{h_{cg}}{b} - \left(1 - \overline{x}_{cg}\right)\vartheta - \overline{y}_{cg}$$

$$\vartheta_T = \vartheta + \Theta_T - \vartheta_0$$

$$f_1 = \frac{1}{m}, \quad f_2 = \frac{\rho S}{2m}, \quad f_3 = \frac{\rho S b}{2J_{xc}}, \quad f_5 = \frac{\rho S b}{2J_{yc}}, \quad f_7 = \frac{\rho S b}{2J_z}, \quad f_8 = \frac{y_T}{J_z}$$

$$f_4 = \left[1 - \frac{J_{xc}}{J_{yc}}\right]\tan\left(\vartheta + \varphi_c - \vartheta_0\right)$$

$$f_6 = \left[1 - \frac{J_{yc}}{J_{xc}}\right]\tan\left(\vartheta + \varphi_c - \vartheta_0\right)$$

$$\varphi_c = \frac{1}{2}\arctan\left[\frac{2J_{xy}}{J_y - J_x}\right]$$

$$J_{xc} = J_x\cos^2\varphi_c + J_y\sin^2\varphi_c - 2J_{xy}\cos\varphi_c\sin\varphi_c$$

$$J_{yc} = J_y\cos^2\varphi_c + J_x\sin^2\varphi_c - 2J_{xy}\cos\varphi_c\sin\varphi_c$$

Since this paper only deals with longitudinal stability, the full motion system can be reduced to the following three equations:

$$\dot{U}_d = f_1 T - f_2 U_a^2 C_x - f_1 R_{x,hydr}(t) \tag{2}$$

$$\dot{U}_{ycg} = f_2 U_a^2 C_y + f_1 T\vartheta - 9.81 + f_1 R_{y,hydr}(t) \tag{3}$$

$$\dot{\omega}_z = \left(f_7 U_a^2 m_z - \frac{y_T}{J_z} T \right) + \frac{m_{z,hydr}(t)}{J_z} \tag{4}$$

Here, $hydr$ stands for hydrodynamics.

2.3 Aerodynamics

The coefficients of aerodynamic forces can be represented as (see Zhukov, 1993):

$$\begin{aligned} C_x &= C_x(\vartheta, h) + C_x^{\dot{\vartheta}}(\vartheta, h)\, \omega_z \frac{b}{U_a} + C_x^{\dot{h}}(\vartheta, h) \frac{U_y}{U_a} \\ C_y &= C_y(\vartheta, h) + C_y^{\dot{\vartheta}}(\vartheta, h)\, \omega_z \frac{b}{U_a} + C_y^{\dot{h}}(\vartheta, h) \frac{U_y}{U_a} \end{aligned} \tag{5}$$

$$m_z = m_z(\vartheta, h) + m_x^{\dot{\vartheta}}(\vartheta, h)\, \omega_z \frac{b}{U_a} + m_x^{\dot{h}}(\vartheta, h) \frac{U_y}{U_a} \tag{6}$$

The determination of aerodynamic characteristics of air wings in semi-connected coordinate system is performed using the programme Autowing.

2.4 Hydrodynamics

For calculation of hydrodynamic forces on a planing part of the boat, a simple strip model proposed by Kovrizhnykh (1978) and described in details by Lotov (1984) is applied. The derivation of Kovrizhnykh starts from Newton's second law for the local force f acting on a cross-section of the planing surface:

$$f = \left(m_{hydr} U_n \right) \frac{d\alpha}{dt}$$

where U_n is the vertical velocity of the cross-section. Integrating the last equation over the whole wetted length, one obtains the total lifting force acting on the hull. Taking into account that the hydrodynamic added mass for a prismatic shaped hull is:

$$m_{hydr} = k(\beta) \rho_W h_1^2$$

the local force can be written in the form:

$$\begin{aligned} f &= \rho_W k(\beta) \left(h_1^2 U_n \right) \frac{d\alpha}{dt} \\ &= \rho_W k(\beta) \left(2 h_1 \dot{h}_1 U_0 + h_1^2 \dot{U}_n \right) \end{aligned} \tag{7}$$

Here, h_1 is a local submergence of the cross-section as a function of the longitudinal coordinate ξ and the unsteady angle of trim $\alpha = \vartheta_0 + \vartheta$, where ϑ_0 is the mean trim angle and ϑ is increment with *respect* to ϑ_0,

$$h_1 = \left(l - \xi_0 - \xi \right) \alpha,$$

ξ_0 is the length between the stern and the LCG. Expressing U_n through $\dot{h}$:

$$\begin{aligned} U_n &= \dot{h}_1 = U_0\alpha - \dot{y} - \xi\dot{\vartheta} \\ \dot{U}_n &= 2U_0\dot{\vartheta} - \ddot{y} - \xi\ddot{\vartheta} \end{aligned} \tag{8}$$

and substituting (8) into (7) gives:

$$\begin{aligned} f(\xi) = \rho_W k(\beta)\Big[& 2\left(l-\xi_0-\xi\right)\alpha\left(U_0\alpha - \dot{y} - \xi\ddot{\vartheta}\right)^2 \\ & + \left(2-\cos(\beta)\right)\alpha^2\left(l-\xi_0-\xi\right)^2\left(2U_0\dot{\vartheta} - \ddot{y} - \xi\ddot{\vartheta}\right)\Big] \end{aligned} \tag{9}$$

The factor $\left(2-\cos(\beta)\right)$ is a correction factor proposed by Logvinovich (see Lotov, 1984).

To get the resulting moment and the resulting force, the $f(\xi)$ function has to be integrated over the ship wetted length:

$$\begin{aligned} Y_{hydr} &= \int_{-\xi_0}^{l-\xi_0} f(\xi)\,d\xi \\ m_{z,hydr} &= \int_{-\xi_0}^{l-\xi_0} f(\xi)\xi d\xi \end{aligned} \tag{10}$$

The wetted length l can also be written as:

$$l = l_0 - \frac{y}{\vartheta_0} - \frac{\left(l_0-\xi_0\right)}{\vartheta_0}\vartheta. \tag{11}$$

Therein, the index 0 stands for the steady state value. The wetted length l_0 is calculated as:

$$l_0 = H_0\vartheta$$

where the submergence of the stern H_0 is calculated iteratively from the equilibrium condition at given speed and trim angle (see Section 2.1). Substituting (9) and (11) into (10) allows one to represent the hydrodynamic forces and moments in form of a truncated Taylor series with respect to y, $\dot{y}$, $\ddot{y}$, ϑ, $\dot{\vartheta}$ and $\ddot{\vartheta}$:

$$\begin{aligned} Y_{hydr}\left(y,\dot{y},\ddot{y},\vartheta,\dot{\vartheta},\ddot{\vartheta}\right) &= Y_0 + F^y y + F^{\dot{y}}\dot{y} + F^{\ddot{y}}\ddot{y} + F^{\vartheta}\vartheta + F^{\dot{\vartheta}}\dot{\vartheta} + F^{\ddot{\vartheta}}\ddot{\vartheta} \\ m_{z,hydr}\left(y,\dot{y},\ddot{y},\vartheta,\dot{\vartheta},\ddot{\vartheta}\right) &= M_0 + M^y y + M^{\dot{y}}\dot{y} + M^{\ddot{y}}\ddot{y} + M^{\vartheta}\vartheta + M^{\dot{\vartheta}}\dot{\vartheta} + M^{\ddot{\vartheta}}\ddot{\vartheta} \end{aligned} \tag{12}$$

Coefficients of the series are presented in Table 2.

The hydrodynamic resistance can also be represented in the form of the Taylor series:

$$W = W_0 + W^y y + W^{\vartheta}\vartheta \tag{13}$$

Table 2 Lift and its trim moment on the planing hull

Parameter	*Lift derivatives F*	*Moment derivatives M*
0	$\rho_W k(\beta) U_0^2 l_0^2 \vartheta_0^3$	$\rho_W k(\beta)\left(\frac{l_0}{3}-\xi_0\right) U_a^2 l_0^2 \vartheta_0^3$
h	$-2\rho_W k(\beta) U_a^2 l_0 \vartheta_0^2$	$-2\rho_W k(\beta)\left(\frac{l_0}{2}-\xi_0\right) U_a^2 l_0 \vartheta_0^2$
$\dot{h}$	$-2\rho_W k(\beta) U_a l_0^2 \vartheta_0^2$	$-2\rho_W k(\beta)\left(\frac{l_0}{3}-\xi_0\right) U_a l_0^2 \vartheta_0^2$
$\ddot{h}$	$-\frac{1}{3}(2-\cos(\beta))\rho_W k(\beta) l_0^3 \vartheta_0^2$	$-\frac{1}{3}(2-\cos(\beta))\rho_W k(\beta)\left(\frac{l_0}{4}-\xi_0\right) l_0^3 \vartheta_0^2$
ϑ	$2\rho_W k(\beta)\left(\frac{l_0}{2}+\xi_0\right) U_a^2 l_0 \vartheta_0^2$	$-2\rho_W k(\beta)\xi_0^2 U_a^2 l_0 \vartheta_0^2$
$\dot{\vartheta}$	$2\rho_W k(\beta)\xi_0 U_a l_0^2 \vartheta_0^2$	$-2\rho_W k(\beta)\left(\frac{l_0^2}{12}-\frac{l_0\xi_0}{3}+\xi_0^2\right) U_a l_0^2 \vartheta_0^2$
$\ddot{\vartheta}$	$-(2-\cos(\beta))\rho_W k(\beta)\frac{l_0}{3}\left(\frac{l_0}{4}-\xi_0\right) l_0^2 \vartheta_0^2$	$-(2-\cos(\beta))\rho_W k(\beta)\frac{l_0}{3}\left(\frac{l_0^2}{10}-\frac{l_0\xi_0}{2}+\xi_0^2\right) l_0^2 \vartheta_0^2$

The hydrodynamic moment M_W caused by W is calculated as:

$$M_W = -W(\eta_0 - H) \tag{14}$$

where H is the submergence at the position of the centre of gravity: $H = H_0 - y + \xi_0\vartheta$ and η_0 is the height of the centre of gravity above keel.

The moment can also be represented in a form of the Taylor series:

$$M_W = M_{W0} + M_W^y y + M_W^\vartheta \vartheta \tag{15}$$

The coefficients are given in Table 3. The wetted surface of the hull S_0 can be calculated from:

$$S_0 = \frac{\pi}{2}\frac{H_0^2}{\vartheta_0 \sin\beta}$$

Table 3 Resistance and its trim moment

Parameter	*Resistance derivatives*	*Moment derivatives*
0	$c_W S_0 \frac{\rho_W U_a^2}{2}$	$-c_W \frac{\rho_W U_a^2}{2} S_0(\eta_0 - H_0)$
h	$-c_W \frac{\rho_W U_0^2 S_0}{H_0}$	$c_W \rho_W U_a^2 \frac{S_0}{H_0}\left(\eta_0 - \frac{3}{2}H_0\right)$
ϑ	$-c_W \frac{\rho_W U_0^2}{2} S_0 \frac{H_0 - 2\xi_0\vartheta_0}{H_0\vartheta_0}$	$c_W \frac{\rho_W U_a^2}{2}\frac{S_0}{\vartheta_0}(2H_0 - \eta_0)$

2.5 Stability analysis

Substituting representations (5), (6), (12), (13) and (15) into systems (2), (3) and (4) and using the dimensionless time τ:

$$t = \tau \frac{2m}{\rho S U_0}$$

we obtain the following linearised motion equations (see also Zhukov, 1993):

$$\begin{aligned}
&\Delta \dot{\bar{U}} + a_{11}\Delta \bar{U} + b_{12}\Delta \ddot{\tilde{h}} + a_{12}\Delta \tilde{h} + a_{13}\Delta \vartheta = 0 \\
&a_{21}\Delta \bar{U} - c_{22}\Delta \ddot{\tilde{h}} + b_{22}\Delta \dot{\tilde{h}} + a_{22}\Delta \tilde{h} + c_{23}\Delta \ddot{\vartheta} + b_{23}\Delta \dot{\vartheta} + a_{23}\Delta \vartheta = 0 \\
&a_{31}\Delta \bar{U} + c_{32}\Delta \ddot{\tilde{h}} + b_{32}\Delta \dot{\tilde{h}} + a_{32}\Delta \tilde{h} - c_{33}\Delta \ddot{\vartheta} + b_{33}\Delta \dot{\vartheta} + a_{33}\Delta \vartheta = 0
\end{aligned} \tag{16}$$

The dimensionless parameters are introduced according to the following relations:

$$\Delta \bar{U} = \frac{\Delta U}{U_0};\quad \dot{\vartheta} = \frac{\rho S U_0}{2m}\dot{\tilde{\vartheta}};\quad \ddot{\vartheta} = \left(\frac{\rho S U_0}{2m}\right)^2 \ddot{\tilde{\vartheta}}$$

$$\tilde{h} = hb;\quad \dot{h} = \frac{\rho S U_0 b}{2m}\dot{\tilde{h}};\quad \ddot{h} = \left(\frac{\rho S U_0}{2m}\right)^2 b\ddot{\tilde{h}}$$

The coefficients a_{ij}, b_{ij} and c_{ij} are given in Table 4 where the following dimensionless parameters are used:

$$\mu = \frac{2m_0}{\rho S b};\quad i_z = \frac{J_z}{mb^2};\quad C_T^{\bar{U}} = \frac{2T^U}{\rho U S}$$

$$\kappa = 2\frac{\rho_W}{\rho}k(\beta)\tilde{l}_0^2\frac{b^2}{S}\vartheta_0^2$$

$$\tilde{l}_0 = \frac{l_0}{b};\quad \tilde{H}_0 = \frac{H_0}{b};\quad \tilde{\xi}_0 = \frac{\xi_0}{b};\quad \tilde{\eta}_0 = \frac{\eta_0}{b}$$

According to the procedure of the linear stability analysis, a differentiation operator is introduced:

$$p = \frac{d}{dt},\quad p^2 = \frac{d^2}{dt^2}$$

into system (16). Replacing derivatives of kinematic parameters by p and p^2 and grouping terms proportional to these parameters, one obtains the system of algebraic equations with respect to U, h and ϑ with the determinant:

$$\begin{vmatrix}
p + a_{11} & b_{12}p + a_{12} & a_{13} \\
a_{21} & -c_{22}p^2 + b_{22}p + a_{22} & c_{23}p^2 + b_{23}p + a_{23} \\
a_{31} & c_{32}p^2 + b_{32}p + a_{32} & -c_{33}p^2 + b_{33}p + a_{33}
\end{vmatrix}$$

Table 4 Coefficients of linearised system

Parameter	*a*	*b*	*c*
11	$2C_W \frac{\rho_W}{\rho} - C_T^{\overline{U}} \frac{\rho_W}{\rho} + 2c_x^0$	0	0
12	$C_x^h - 2C_W \frac{\rho_W}{\rho} \frac{S_0}{S} \frac{1}{\tilde{H}_0}$	$C_x^{\dot{h}} \frac{1}{\mu}$	0
13	$C_x^{\vartheta} - C_W \frac{\rho_W}{\rho} \frac{S_0}{S} \frac{\tilde{H}_0 - 2\tilde{\xi}_0 \vartheta_0}{\tilde{H}_0 \vartheta_0}$	0	0
21	$\left(2C_y^0 + C_T^{\overline{U}} \frac{\rho_W}{\rho} \vartheta_T\right)\mu$	0	0
22	0	$C_x^{\dot{h}} - 2\kappa$	$1 + \frac{1}{3}(2 - \cos\beta)\tilde{l}_0 \kappa \frac{1}{\mu}$
23	$\left(C_y^{\vartheta} + 2\kappa\left(\frac{\tilde{l}_0}{2} + \tilde{\xi}_0\right)\frac{1}{\tilde{l}_0}\right)\mu$	$C_y^{\dot{\vartheta}} + 2\kappa\tilde{\xi}_0$	$-(2 - \cos\beta)\kappa \frac{\tilde{l}_0}{3}\left(\frac{\tilde{l}_0}{4} - \tilde{\xi}_0\right)\frac{1}{\mu}$
31	$\left[-\tilde{y}_T \frac{\rho_W}{\rho} C_T^{\overline{U}} + 2\left(C_T^0 \frac{\rho_W}{\rho} - C_W \frac{\rho_W}{\rho} \frac{S_0}{S}(\tilde{\eta}_0 - \tilde{H}_0)\right)\right]\frac{\mu}{i_z}$	0	0
32	$\left(m_z^h - 2\kappa\left(\frac{\tilde{l}_0}{2} - \tilde{\xi}0\right)\frac{1}{\tilde{l}_0} + 2C_W \frac{\rho_W}{\rho} \frac{S_0}{S} \frac{\tilde{\eta}_0 - \frac{3}{2}\tilde{H}_0}{\tilde{H}_0}\right)\frac{\mu}{i_z}$	$\left(m_z^{\dot{h}} - 2\kappa\left(\frac{\tilde{l}_0}{3} - \tilde{\xi}_0\right)\right)\frac{1}{i_z}$	$\left(m_z^{\ddot{h}} - \frac{1}{3}\kappa(2 - \cos\beta)\left(\frac{\tilde{l}_0}{4} - \tilde{\xi}_0\right)\tilde{l}_0\right)\frac{1}{\mu i_z}$
33	$\left(m_z^{\vartheta} - \kappa \frac{\tilde{\xi}_0^2}{\tilde{l}_0} + C_W \frac{\rho_W}{\rho} \frac{S_0}{S} \frac{2\tilde{H}_0 - \tilde{\eta}_0}{\vartheta_0}\right)\frac{\mu}{i_z}$	$\left(m_z^{\dot{\vartheta}} - 2\kappa\left(\frac{\tilde{l}_0^2}{12} - \frac{\tilde{l}_0\tilde{\xi}_0}{3} + \tilde{\xi}_0^2\right)\right)\frac{1}{i_z}$	$1 + \kappa(2 - \cos\beta)\frac{\tilde{l}_0}{3}\left(\frac{\tilde{l}_0^2}{10} - \frac{\tilde{l}_0\tilde{\xi}_0}{2} + \tilde{\xi}_0^2\right)\frac{1}{\mu i_z}$

Calculation of the determinant results in the characteristic equation of system (16):

$$D_5 p^5 + D_4 p^4 + D_3 p^3 + D_2 p^2 + D_1 p + D_0 = 0$$

This equation is quintic and has five roots. All of the real parts of these roots have to be negative for a stable planing.

Necessary and sufficient conditions of stability are (see Zhukov, 1993):

$$D_i > 0, (i = 1, 2, 3, 4, 5); D_1 D_2 - D_3 > 0;$$

$$R_5 = (D_1 D_2 - D_3)(D_3 D_4 - D_2 D_5) - (D_1 D_4 - D_5)^2 > 0$$

The boundary of dynamic (oscillatory) stability is determined by equation $R_5 = 0$ and the boundary of static (aperiodic) stability $D_5 = 0$ with other conditions of stability being fulfilled.

Figure 5 Model for determination of mass moment of inertia I_z

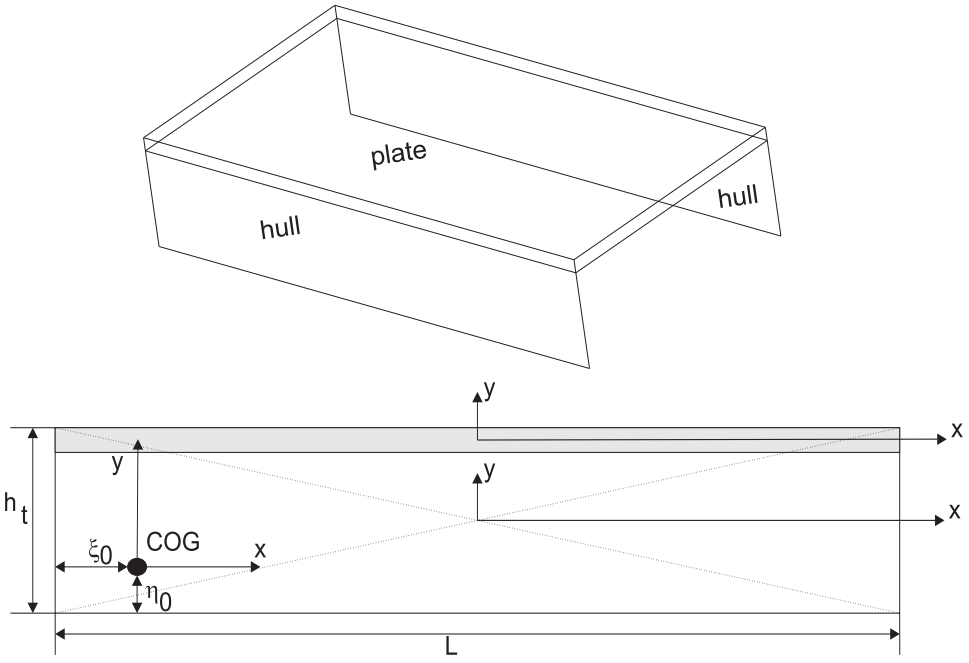

3 Results of the stability analysis

The analysis presented above was implemented into a Fortran programme called STABBI and intended for the longitudinal stability analysis of racing boats with aerodynamic support. Because of lack of information on the mass moment of inertia, it was calculated under assumption that the planing boat consist of three parts, two hulls and the wing between them. They are modelled as flat rectangular plates with uniform

mass distribution on areas $S_{wing} = Lb$ and $S_{hull} = L \cdot h_t$. Figure 5 shows this geometric model and three different coordinate systems. For a plate, the mass moment of inertia around the lateral axis is defined as:

$$J_z = \int \left(x^2 + y^2\right) dm$$

The mass moment of inertia J_z can be transferred to the coordinate system of the craft with the origin in the centre of gravity by Steiners theorem. This results in:

$$J_z = \frac{2}{12} m_{hull} \left(L^2 + h_t^2\right) + \frac{1}{12} m_{plate} L^2 + 2 m_{hull} \left(\left(\frac{L}{2} - \xi_0 \right)^2 + \left(\frac{h_t}{2} - \eta_0 \right)^2 \right)$$
$$+ m_{plate} \left(\left(\frac{L}{2} - \xi_0 \right)^2 + \left(h_t - \eta_0 \right)^2 \right)$$

The mass of the hull part and the wing is then calculated by:

$$m_{hull} = \frac{S_{hull}}{S_{hull} + S_{wing}} m$$

$$m_{wing} = \frac{S_{wing}}{S_{hull} + S_{wing}} m$$

The influence of the following kinematic and geometric parameters of the racing boats on stability was studied:

- γ [deg] – setup angle of the air wing with respect to the planing surface
- β [deg] – deadrise angle of the planing surface
- b [m] – chord of the air wing
- L [m] – span of the air wing between end plates
- ξ_0 and η_0 [m] – coordinates of the centre of gravity measured from the transom and the planing surface
- h_t [m] – height of the racing boat at the transom
- m [kg] – mass
- J_z [k/gm^2] – mass moment of inertia
- U [m/sec] – speed of motion.

Based on these parameters, the following dimensionless parameters can be proposed for further investigations of the stability:

$$\gamma\ ;\ \beta\ ;\ \tilde{\xi}_0 = \frac{\xi_0}{b}\ ;\ \tilde{\eta}_0 = \frac{\eta_0}{b}\ ;\ \mu = \frac{2m_0}{\rho S b}$$

$$i_z = \frac{J_z}{m_0 b^2};\ \lambda = \frac{L}{b};\ \tilde{h}_t = \frac{h_t}{b};\ \tilde{U} = \frac{U}{\sqrt{\frac{m_0 g}{\rho L b}}}$$

The dimensionless parameters were varied in the range typical for modern racing boats (see Table 5).

Table 5 Standard parameter (dimensional and non-dimensional)

Parameter	*Value*	*Parameter*	*Value*
m	4,800 kg	μ	33
J_z	74,436 kgm^2	i_z	0.108
γ	0 deg	β	20
b	12 m	$\tilde{\xi}$	0.35
L	2 m	$\tilde{\eta}$	0.083
ξ	4.2 m	λ	0.166
η	1 m	h_t	0.0542
h_t	0.65 m		

Study of the stability has been performed for two cases. In the first case (see Figures 6 to 13), the velocity U and the trim are given, whereas the submergence of the boat is found from the condition that the lift is equal to the boat weight. It is supposed that the given trim angle can be secured by trim tabs, flaps or spoilers, whereas the speed is achieved by proper choice of the engine. Results of such a study can be used for design of new boats when the designer is free to change the hull form. The second case (see Figure 14) concerns the situation when some parameters of already existing boats are changed and influence the stability. A usual case is the shift of the centre of gravity, which results in the change of both trim and submergence. Stability results in this case are different from that when the trim is specified (see Figure 9).

The diagrams of stability were obtained by variation of the speed and the trim angle. The curves of the diagrams show the border between stable and unstable planing. Beneath each curve, the planing is stable at a given speed U and trim angles ϑ, whereas above the line, it is unstable. The stability decreases with increasing speed because aerodynamic and hydrodynamic lifts are getting larger and the submerged part of the hull contributing to the stability becomes smaller. The same effect takes place when the trim angle increases.

For the following investigations, a boat with the parameters shown in Table 5 was used.

Concerning the contribution of the air wing to the stability, it was found that this contribution is usually negative. Figure 6 illustrates this fact. This happens because the submerged part of the boat becomes smaller and a larger part of the boat weight is carried by the air wing which is unstable. In fact, the stability of WIG effect craft is secured mostly by the large tail unit. The WIG wing alone is unstable. The area of the stability of the boat with an air wing is smaller than that of the boat consisting only planing part.

Only at small speed U when the influence of the aerodynamics is negligible the stability is the same for both boats.

Figure 7 shows the diagram in which the value of μ was varied. For a small μ, the area of stable planing is also small. When μ rises, the stability gets better. Increase of μ is affected by an increase of the submerged part of the boat which contributes to the stability. Therefore, increase of the mass helps to avoid porpoising instability.

The diagram in Figure 8 shows the stability regime for different deadrise angles β. Increase of the deadrise angle β influences stability in the same way as the dimensionless mass increase. When β gets larger, the area of stable planing also increases.

Figure 9 shows the diagram illustrating the influence of the longitudinal position of the centre of gravity at a given trim. The largest area of stability is observed at the smallest value of $\tilde{\xi}$. When the LCG is moved aft and $\tilde{\xi}$ is decreased, the area of pitch angles corresponding to the stability becomes larger.

The diagram in Figure 10 shows that a change of $\tilde{\eta}$ does not influence the longitudinal stability very much (but it is well-known to be important for lateral instability). For different $\tilde{\eta}$, the border curves between stable and unstable planing are nearly the same.

The height of the boat at the transom determines the largest flight height for the racing boat without loosing contact with the water surface. The diagram in Figure 11, in which the parameter $\tilde{h}_t$ is varied, shows no significant change of stability for different heights of the transom.

The results of the stability estimations show (see Figure 12) that the stability area for different mass moments of inertia i_z is almost the same. It has to be noted that there were no reliable information on this parameter available. It might be that the real mass moment lies outside of the range investigated in this paper. Therefore, this parameter has to be investigated more thoroughly in future works.

Figure 13 shows that the aspect ratio λ of the air wing has an important influence on stability. With increasing λ (increase of the span at constant chord), the stability area decreases significantly. Increasing the aspect ratio leads to an increase of aerodynamic forces which in turn reduces the submerged hull hydrodynamic forces that enhance stability.

The results presented in Figure 14 are obtained by taking the change of both trim and submergence caused by shift of the centre of gravity into account. The pitch angle and the submergence are found from two equations obtained from balance of forces and moments. The equilibrium conditions when the vessel is free to trim and sink lie below the limits of the stability calculated for a LCG at a given trim (see Figure 9), i.e., all investigated conditions are stable ones. Increase in speed causes a decrease of the pitch angle. At each speed, a forward shift of the centre of gravity results in the decrease of the pitch angle. At a glance it should contribute to the stability. However, a more detailed analysis shows that the distance between the equilibrium point and the border of the stability is nearly the same for all positions of the centre of gravity. Moreover, the magnitude of the largest negative root which can be considered as a stability measure is almost the same for all positions. Therefore, the present analysis shows that the position of the centre of gravity does not influence the stability for the given ship configuration. A similar conclusion has been drawn in WIG stability theory (see Zhukov, 1993) where it

has been shown that the mutual position of two aerodynamic centres is important and not the position of the centre of gravity.

Figure 6 Stability with and without aerodynamic support

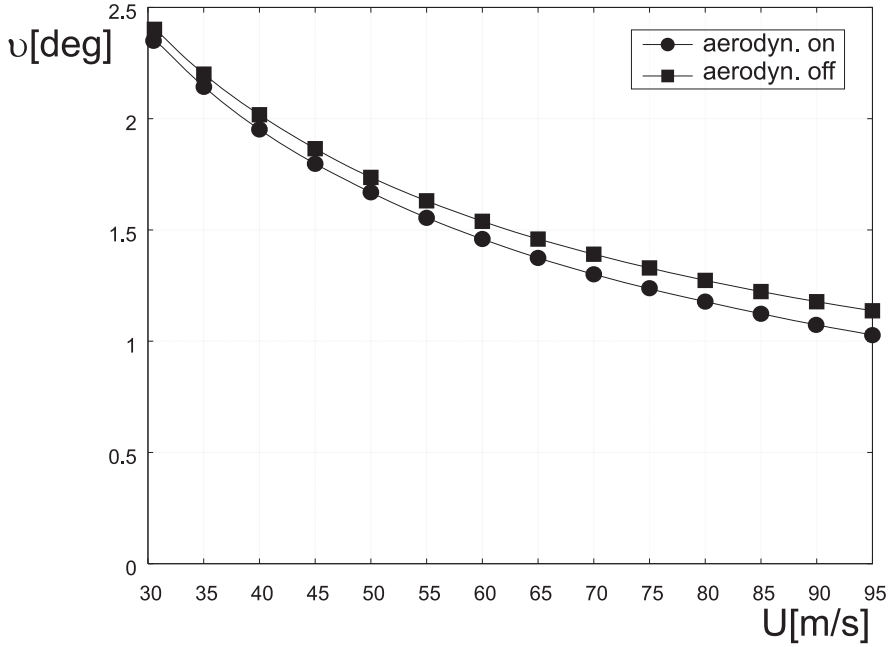

Figure 7 Influence of dimensionless mass μ on stability

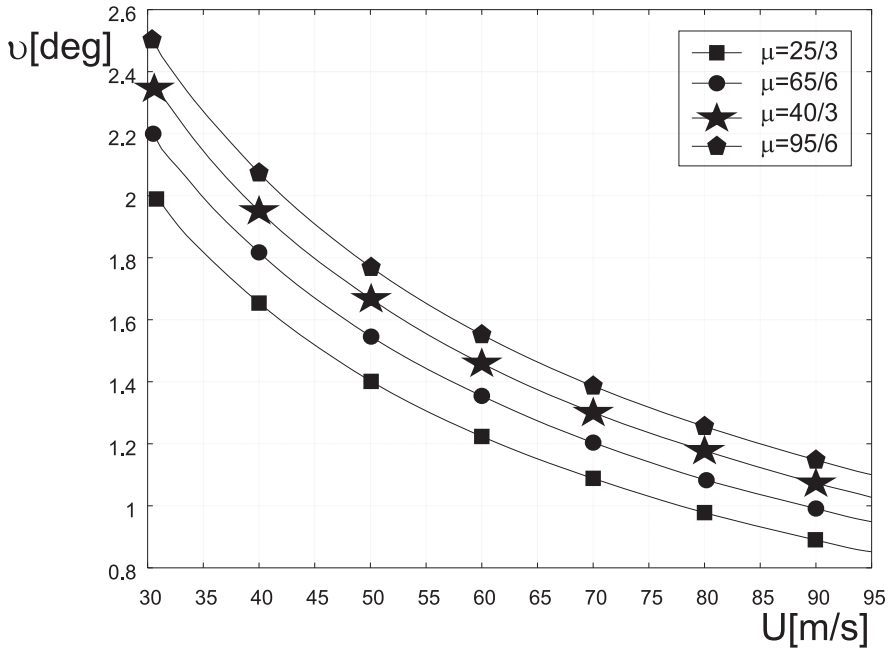

Figure 8 Influence of deadrise angle β on stability

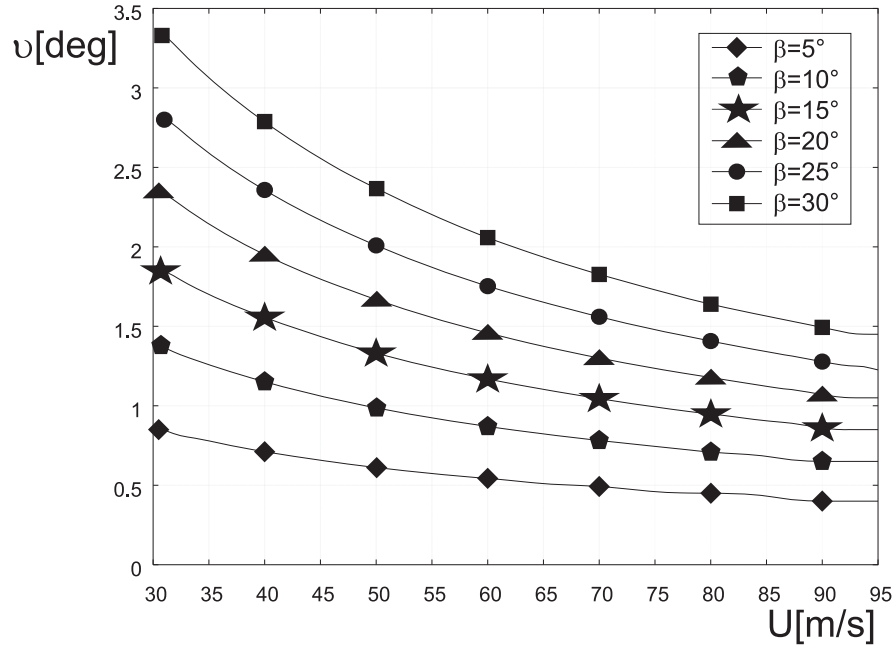

Figure 9 Influence of dimensionless LCG $\tilde{\xi}$ on stability at given trim

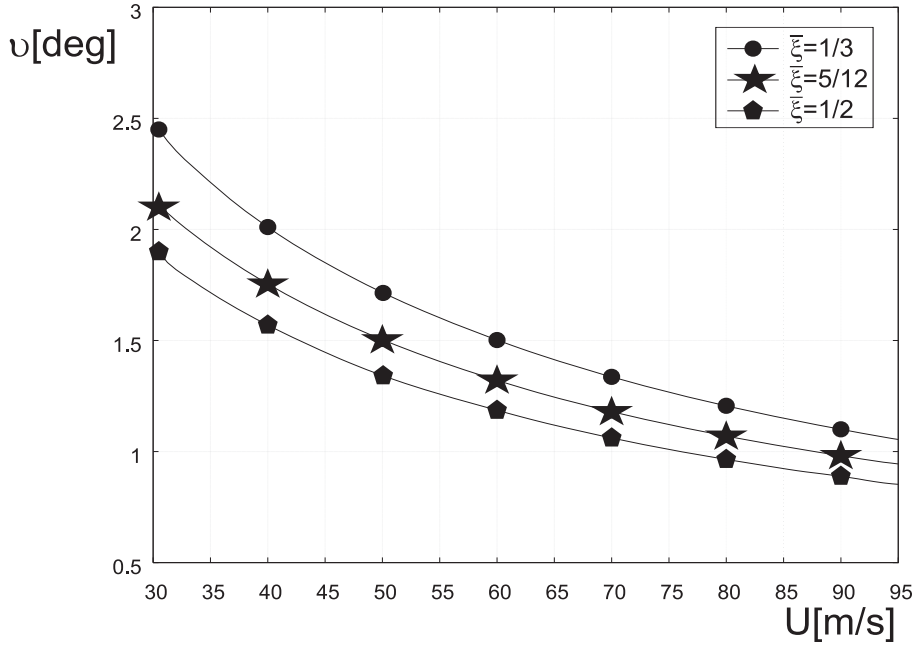

Figure 10 Influence of dimensionless vertical centre of gravity $\tilde{\eta}$ on stability

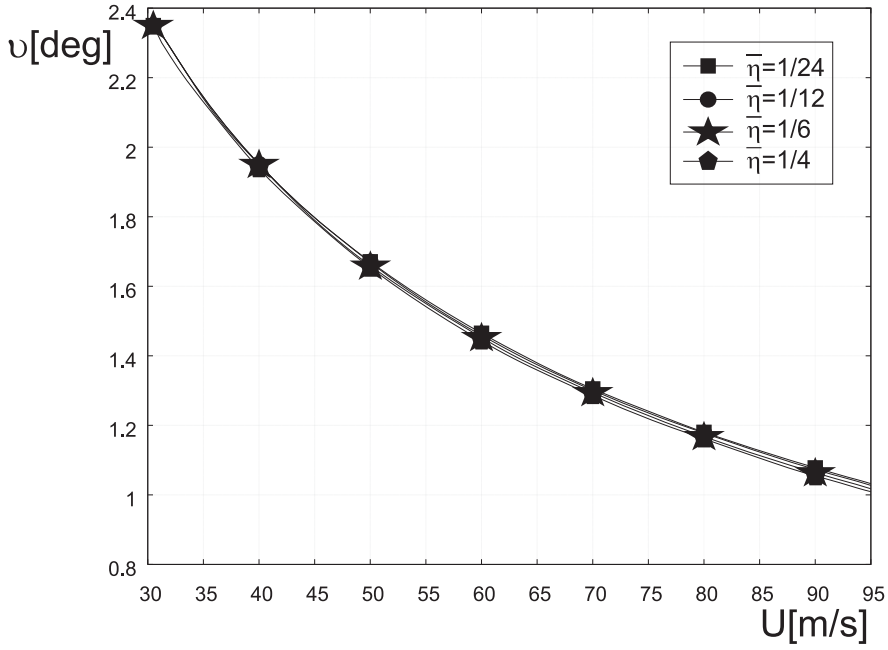

Figure 11 Influence of dimensionless height of the boat at transom $\tilde{h}_t$ on stability

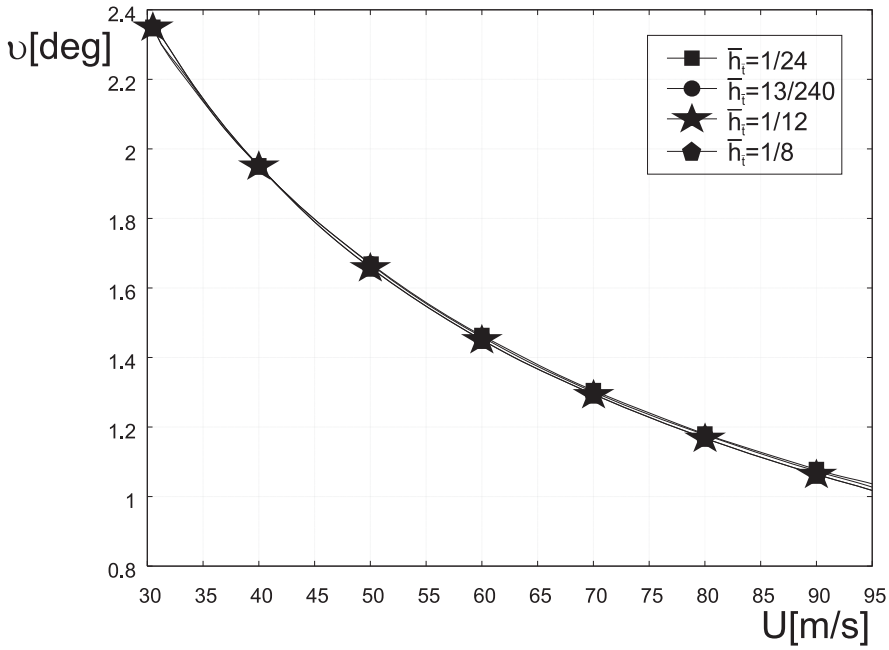

Figure 12 Influence of dimensionless mass moment of inertia i_z on stability

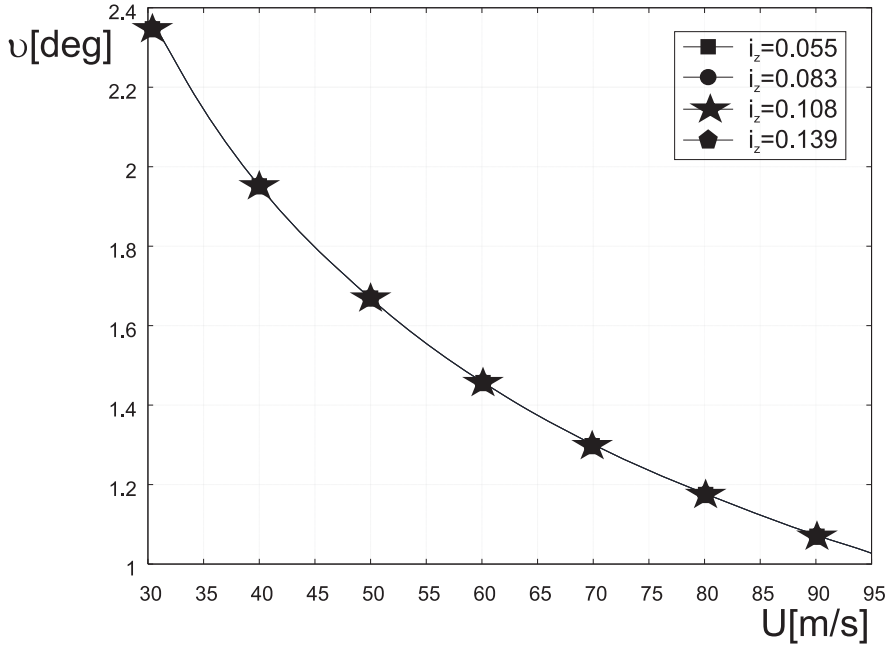

Figure 13 Influence of aspect ratio λ on stability

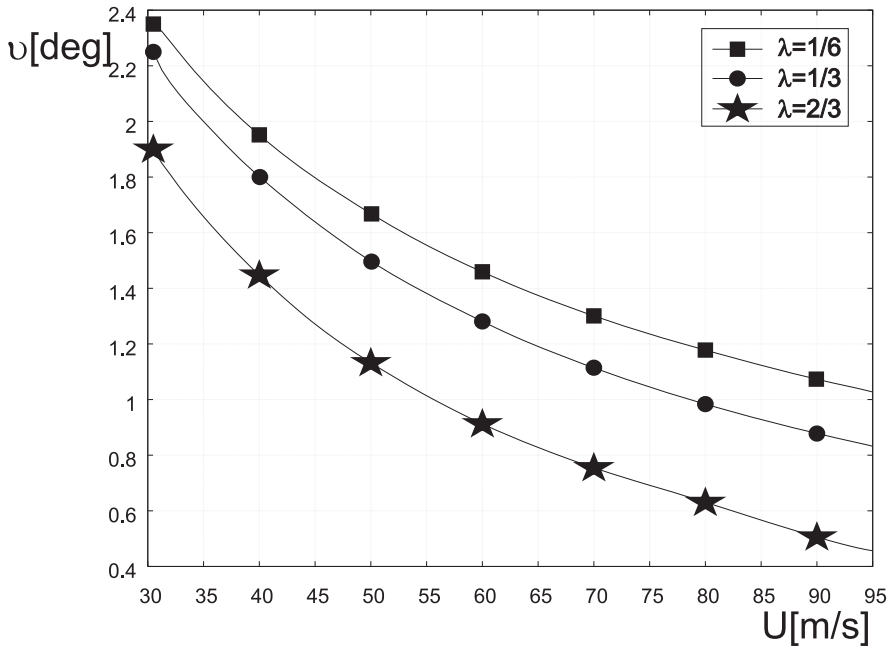

Figure 14 Influence of dimensionless LCG $\tilde{\xi}$ on stability

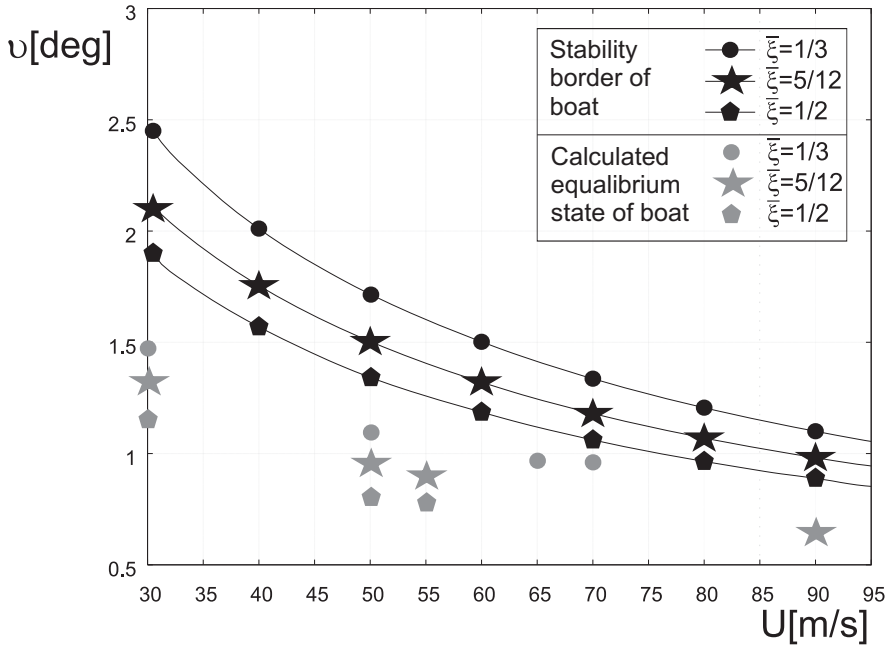

4 Conclusions

A mathematical model and corresponding computer programme has been developed to estimate the longitudinal stability of racing boats with aerodynamic support. It was shown that the aerodynamic forces acting on racing boats contribute to the dynamic instability. The stability can be sufficiently improved by increase of the deadrise angle and dimensionless mass.

Influence of the vertical position of the centre of gravity, height of the boat at the transom and mass moment of inertia is negligible. Increase of the aspect ratio of air wings enhances instability. The present analysis shows that the position of the centre of gravity does not influence the stability for the given ship configuration.

References

Benedikt, K., Kornev, N.V., Meyer, M. and Ebert, J. (2001) 'Complex mathematical model of the WIG motion including the take-off mode', *Journal of Ocean Engineering*, Vol. 29, No. 3, pp.315–357.

Englar, R.B., Gregory, S.D. and Ford, D.A. (1995) 'In ground effect evaluation and aerodynamic development of advanced unlimited racing hydroplanes', *AIAA Aerospace and Sciences Meeting and Exhibit*, 9–12 January, AIAA 1995-745.

Irodov, R.D. (1970) 'Criteria of longitudinal stability of ekranoplan', *Technical Note of the Central Hydro-Aerodynamical Institute (TSAGI)*, Vol. 1, No. 4, in Russian.

Kornev, N., Kleinsorge, L. and Migeotte, G. (2008) 'Dynamics and stability of racing boats with air wings', *Proceedings of the 6th International Conference on High Performance Marine Vehicles*, Italy.

Kovrizhnykh, L.D. (1978) 'Stability of planing of a plate with deadrise angle on the incomplete width', *Proceedings of the Central Hydro-Aerodynamical Institute (TSAGI)*, No. 1972, pp.15–24.

Lotov, V.B. (1984) 'Planing and impact problems', *Textbook of the Moscow Institute of Applied Physics*.

Morch, H.J.B. (2003) 'Aerodynamic properties of an offshore racing catamaran', *FAST03*, Southhampton, UK.

Plisov, N.B., Rozhdestvensky, K.V. and Treshkov, V.K. (1991) 'Aerohydrodynamics of ships with dynamic principles of support', *L., Sudostroenie*, p.248.

Russel, J. (2007) *Secrets of Tunnel Boat Design 2007*, available at http://www.aeromarineresearch.com.

Staufenbiel, R.W. (1987) 'On the design of stable ram wing vehicles', *Proceedings of the Ram Wing and Ground Effect Conf.*, 19 May.

The Specialist Committee of High-Speed Marine Vehicles (2001) *Final Report and Recommendations to the 22nd ITTC*.

Tikhonov, A.N. (1961) 'Determination of the stability area for the planning plates with deadrise angle', *Technical Proceedings of the Central Hydro-Aerodynamical Institute (TSAGI)*, Vol. 202, in Russian.

Zhukov, V.I. (1993) 'Peculiar features of dynamics of ekranoplan', *Proceedings of the First International Conference on Ekranoplans*, St. Petersburg, pp.23–36.